Neurobiology of Aging 129 (2023) 62–71

Contents lists available at ScienceDirect

Neurobiology of Aging

journal homepage: www.elsevier.com/locate/neuaging.org

Nigrostriatal 6-hydroxydopamine lesions increase alpha-synuclein levels and permeability in rat colon

Hengjing Cui [a], Joshua D. Elford [b], Okko Alitalo [a,1], Paula Perez-Pardo [b], Janne Tampio [a], Kristiina M. Huttunen [a], Aletta Kraneveld [b], Markus M. Forsberg [a], Timo T. Myöhänen [a], Aaro J. Jalkanen [a,*]

[a] School of Pharmacy, University of Eastern Finland, Kuopio, Finland
[b] Utrecht Institute of Pharmaceutical Sciences, Utrecht University, Helsinki, the Netherlands

ARTICLE INFO

Article history:
Received 8 February 2023
Revised 25 April 2023
Accepted 3 May 2023
Available online 7 May 2023

Keywords:
Parkinson's disease
Alpha-synuclein
6-hydroxydopamine
Lesion
Rat
Colon

ABSTRACT

Increasing evidence suggests that the gut–brain axis plays a crucial role in Parkinson's disease (PD). The abnormal accumulation of aggregated alpha-synuclein (aSyn) in the brain is a key pathological feature of PD. Intracerebral 6-hydroxydopamine (6-OHDA) is a widely used dopaminergic lesion model of PD. It exerts no aSyn pathology in the brain, but changes in the gut have not been assessed. Here, 6-OHDA was administered unilaterally either to the rat medial forebrain bundle (MFB) or striatum. Increased levels of glial fibrillary acidic protein in the ileum and colon were detected at 5 weeks postlesion. 6-OHDA decreased the Zonula occludens protein 1 barrier integrity score, suggesting increased colonic permeability. The total aSyn and Ser129 phosphorylated aSyn levels were elevated in the colon after the MFB lesion. Both lesions generally increased the total aSyn, pS129 aSyn, and ionized calcium-binding adapter molecule 1 (Iba1) levels in the lesioned striatum. In conclusion, 6-OHDA-induced nigrostriatal dopaminergic damage leads to increased aSyn levels and glial cell activation particularly in the colon, suggesting that the gut–brain axis interactions in PD are bidirectional and the detrimental process may start in the brain.

1. Introduction

Parkinson's disease (PD) is the second most common neurodegenerative disease and the most common movement disorder (Simon et al., 2020). In addition to the well-characterized motor impairments that arise from the depletion of dopamine in the caudate putamen and the degeneration of dopaminergic neurons in the substantia nigra (SN), several nonmotor symptoms are common in PD, such as constipation, sleep disorders, hyposmia, and, in the later stages of the disease, depression and psychosis. With the progression of the disease, both motor and nonmotor symptoms worsen, resulting in disability and a significant reduction in the patient's quality of life. However, still today, PD treatment is based on dopamine replacement therapy, and disease-modifying therapies have not reached clinical use. Therefore, it is essential to study the pathophysiological mechanisms underlying PD if one wishes to develop novel disease-modifying therapies and identify novel diagnostic biomarkers.

Certain nonmotor symptoms are thought to precede movement disorders by as much as 10–20 years (Klingelhoefer and Reichmann, 2015). One such presymptom is constipation, which has raised substantial interest in the role of the gut–brain axis in PD. There are numerous reports that PD patients exhibit changes in the composition and function of their gut microbiome (Boertien et al., 2022; Keshavarzian et al., 2015; Scheperjans et al., 2015). Another finding that supports the role of the gut–brain axis in PD is the putative propagation of aggregated alpha-synuclein (aSyn) and Lewy bodies via the vagus nerve to the brain as hypothesized in 2003 by Braak et al. (2003). Although the role of propagation in the clinical setting is not fully understood, in some studies, an increased accumulation of aSyn has been observed in the gut of PD patients (Pouclet et al., 2012), but others have failed to confirm this finding (Antunes et al., 2016). However, preclinical models have shown that patient-derived aSyn (Holmqvist et al., 2014) and fibrillar aSyn (Kim et al., 2019) can indeed

Abbreviations: 6-OHDA, 6-hydroxydopamine; aSyn, alpha-synuclein; CNS, central nervous system; GFAP, glial fibrillary acidic protein; Iba-1, ionized calcium-binding adapter molecule 1; MFB, medial forebrain bundle; MPTP, 1-methyl-4-phenyl-1,2,3,6-tetrahydropyridine; PD, Parkinson's disease; pS129 aSyn, alpha-synuclein phosphorylated at serine 129; SN, substantia nigra; STR, striatum; TH, tyrosine-hydroxylase; ZO-1, Zonula occludens protein 1

* Correspondence to: School of Pharmacy, University of Eastern Finland, PO BOX 1627, FI-70211 Kuopio, Finland.
E-mail address: aaro.jalkanen@uef.fi (A.J. Jalkanen).
[1] Current address: Laboratory of Neurotherapeutics, Division of Pharmacology and Pharmacotherapy, Faculty of Pharmacy, University of Helsinki, Finland.

https://doi.org/10.1016/j.neurobiolaging.2023.05.007

be transferred from the gut to the brain and evoke neuronal toxicity in the SN. In mice, aSyn propagation and toxicity were blocked by vagotomy, supporting the role of the vagus nerve in the spreading of aSyn to the brain, and a register study from a Swedish cohort indicated the protective role of truncal vagotomy against PD (Liu et al., 2017). However, there is also recent evidence from animal model studies that aSyn can propagate from the gut to other organs such as the skin and heart via sympathetic nerves (Van Den Berge et al., 2019, 2021). In addition, there is accumulating evidence that inflammation and alterations in the immune system are present in PD pathophysiology [for a comprehensive review, see Tansey et al. (2022)]. Interestingly, chronic inflammatory gut diseases increase the risk for PD (Zhu et al., 2022), and it is possible that inflammatory processes induce a state of aSyn instability in the gut and increase the leakage of reactive glial cells into the brain. However, already, Braak et al. observed that not all PD patients have Lewy bodies arising via the vagus nerve, and the connection between gut inflammation and PD has not been verified in all studies (Mertsalmi et al., 2021). Therefore, it has been suggested that PD could have two subsets, the first being "body-first" PD and the second "brain-first" PD, depending on where the pathology has initiated (Horsager et al., 2020).

The role of the gut in PD can be modeled in preclinical settings, for example, by injecting aSyn preformed fibrils into the duodenum and stomach mucosa (Challis et al., 2020; Kim et al., 2019; Van Den Berge et al., 2019, 2021). Moreover, in aSyn transgenic mice, enteric inflammation and gut leakage have been observed before the appearance of motor symptoms (Pellegrini et al., 2022). Oral administration of rotenone, a toxin model of PD, was observed to increase the amounts of inflammatory markers and aSyn in the colon of mice (Dodiya et al., 2020; Perez-Pardo et al., 2019) and systemically injected 1-methyl-4-phenyl-1,2,3,6-tetrahydropyridine (MPTP)-induced aSyn oligomerization and intestinal dysfunction (Li et al., 2020; Shan et al., 2021). Interestingly, even nigral injection of a widely used toxin, 6-hydroxydopamine (6-OHDA), evoked changes in gut neurotransmitter levels, particularly in acetylcholine (Garrido-Gil et al., 2018), and caused intestinal dysfunction (Toti and Travagli, 2014) and mild enteric neuropathy (McQuade et al., 2021). This suggests that pathogenic events can also move from the brain to the gut, and at least, aSyn has been shown to transfer from the brain to the stomach (Ulusoy et al., 2017).

6-OHDA causes a rapid depletion of nigrostriatal tyrosine-hydroxylase positive (TH+) neurons after the injection of the toxin into the rat or mouse SN or medial forebrain bundle (MFB), mimicking the end-stage of PD (El-Gamal et al., 2021). It can also be delivered as a striatal injection, causing a more progressive and less severe partial lesion in nigrostriatal TH+ nerves and a less extensive depletion of striatal dopamine levels. While 6-OHDA causes severe neuronal inflammation in the brain, it does not lead to any aSyn aggregation. However, if there is a lack of aSyn, this reduces the toxicity of 6-OHDA, suggesting that aSyn is also involved in this toxin model (Alvarez-Fischer et al., 2008). As studies suggested that intracerebral 6-OHDA can induce alterations in gut functions, we have characterized these and assessed the changes in inflammation markers in the gut and other markers related to PD. To our surprise, not only did we observe an increase in glial fibrillary acidic protein (GFAP), a marker for astroglial cells, but we also noted an increase in total and Ser129 phosphorylated aSyn levels in the colon and increased colonic permeability after the MFB lesion. Our results suggest that pathophysiological events occurring in the brain can induce several pathological features connected to PD in the gut.

2. Materials and methods

2.1. Animals

Male RccHan:Wistar rats supplied by the Laboratory Animal Center of the University of Eastern Finland were used in the studies. The rats were 11–12 weeks old and weighed 310–370 g at the beginning of the experiments. The animals were group-housed (except for 2 days postsurgery to ensure wound healing) and kept on a 12-hour light/12-hour dark cycle (lights on between 7 AM and 7 PM) at an ambient temperature of 22 ± 1 °C. Pelleted food (Teklad 2016, Envigo, The Netherlands) and tap water were available ad libitum. All procedures with the animals were conducted in accordance with the "Principles of Laboratory Animal Care" (NIH publication #85–23, revised in 1985) and the European Commission Directive 2010/63/EU and approved by the Finnish National Animal Experiment Board (license ESAVI-2014-701). All efforts were made to minimize the number of animals used and their suffering.

2.2. 6-OHDA lesions

Intracerebral 6-OHDA administration was conducted as previously described by Leikas et al. (2017). The rats were randomly assigned into three groups: (1) sham (i.e., sham lesioned, n = 4), (2) STR (10 µg of 6-OHDA into the striatum, i.e., a partial lesion, n = 7), and (3) MFB (10 µg of 6-OHDA into the medial forebrain bundle, i.e., a full lesion, n = 7). Briefly, the rats were first anesthetized with sodium pentobarbital (60 mg/kg i.p.; Mebunat Vet, Orion Oyj, Espoo, Finland) and attached to a stereotaxic frame. Thirty minutes before the surgery and 6 hours after the surgery, buprenorphine (0.02 mg/kg s.c.; Temgesic, Schering-Plough, Kenilworth, NJ, USA) was given to relieve any postoperative pain. Next, the skull was exposed, a small hole was drilled into the skull above the desired brain area, and 10 µg of 6-OHDA as a free base (Sigma; dissolved in 0.9% NaCl containing 0.2 mg/ml of ascorbic acid) was infused over an 8-minute period at a flow rate of 0.5 µl/min into the brain. The final coordinates (from the bregma as calculated from the top of the skull) for the partial striatal lesions (group STR) were AP +1.0, L −2.7, and DV −5.0 and for the full lesions (group MFB) AP −4.4, L −1.2, and DV −8.3. Following the 8-minute infusion, the needle was left in place for an additional 4 minutes to prevent toxin backflow. Sham-lesioned animals were operated exactly as the MFB-lesioned rats, but only 4 µl of vehicle (0.9% NaCl containing 0.2 mg/ml of ascorbic acid) was infused into the MFB. The wound was closed with 2 stitches, and the animals were allowed to recover from the surgery in individual cages for 2 days, after which they were returned into groups of 3–4 animals per cage.

2.3. Behavioral studies

Four weeks after the 6-OHDA lesioning, the rats were subjected to a series of sensorimotor behavioral tests to evaluate the success of the lesion and the behavioral deficits caused by the unilateral 6-OHDA infusions. The test battery assessed the different domains of forelimb use in tasks requiring skilled and coordinated motor functions, and it consisted of the cylinder, the adjusting steps, the movement initiation, and the vibrissae tests (Leikas et al., 2017). The ipsilateral limb use preference (i.e., the ability to use the forelimb ipsilateral to the site of the 6-OHDA lesion) was assessed in each test. The researcher conducting the behavioral tests and scoring was blind to the experimental groups. In the cylinder test, the rats were placed into a clear cylinder (Ø 20 cm, height 30 cm) and were allowed to freely explore the cylinder for 3 minutes. Each trial was recorded, and from the captured video, the touches of the ipsilateral, contralateral, and both forelimbs during the vertical exploration along the cylinder walls were scored. The ipsilateral limb use preference was calculated with the equation (ipsilateral/[ipsilateral + contralateral + both]) − (contralateral/[ipsilateral + contralateral + both]). The adjusting step tests evaluated the forelimb use in a situation where the researcher held the rat by its torso above a table and allowed the rat to bear its body weight on one forelimb.

The rat was then moved laterally along the tabletop, and the number of adjusting steps for both the ipsilateral and contralateral forelimbs was recorded over an 80 cm distance. Both forehand and backhand directions were investigated in 5 consecutive trials, the results were averaged, and the ipsilateral preference was calculated with the equation (ipsilateral/[ipsilateral + contralateral]) – (contralateral/[ipsilateral + contralateral]). In the movement initiation test, the rat was held similarly to the adjusting steps test, but, instead of a lateral movement, the rat was gently pushed forward, and the length of the correcting step was recorded for both forelimbs. The test was repeated 5 times, and the average step lengths were used in the calculation of the ipsilateral limb use preference by the equation (ipsilateral/[ipsilateral + contralateral]) – (contralateral/[ipsilateral + contralateral]). In the vibrissae test, the rat was held by its torso, and the vibrissae were brushed against the table surface. The ability of the rat to react to the stimulus was assessed by calculating the number of successful forelimb placements on the tabletop in 10 consecutive trials. The ipsilateral limb use preference was calculated with the equation (ipsilateral/[ipsilateral + contralateral]) – (contralateral/[ipsilateral + contralateral]). Finally, an overall ipsilateral limb use score was calculated as an average score combining the scores from each test.

2.4. Sample collection

Five weeks after the 6-OHDA or sham lesion, the animals were killed by brief CO_2 exposure and decapitation. The brains were quickly removed, and the left and right striatum and the medial prefrontal cortex were dissected and snap-frozen in liquid nitrogen to be used in western blot analyses. The intestines were exposed, and about 5-cm-long segments of the distal ileum and proximal colon were dissected for immunohistochemistry. Separate, approximately 1-cm-long intestinal samples were collected, gently washed with phosphate-buffered saline (PBS), and frozen in liquid nitrogen. These samples were later used in the western blot analyses.

2.5. Immunohistochemistry

The intestinal segments for the immunohistochemical staining were prepared using the Swiss roll method. The 5-cm-long segments were washed with 10 ml of Bouin's fixative (containing 50% v/v ethanol and 5% v/v acetic acid in H_2O) using a syringe and a needle. Next, the segments were cut longitudinally along the mesenteric line and rinsed with PBS. Then, the segments were placed with the luminal side facing upward and wrapped around a wooden toothpick to form a Swiss roll. Finally, the rolls were allowed to incubate overnight in 10% buffered formalin at room temperature and stored at −80 °C until the immunohistochemical staining.

Upon thawing, the Swiss rolls of the colon and ileum were embedded in paraffin, and 5-μm cross-sections of complete intestines were taken. Following this, the samples were incubated in 0.3% H_2O_2 for 30 minutes and rehydrated, and antigen retrieval was performed using citrate buffer. Incubation with primary antibodies (Table 1) was then performed overnight at 4 °C. After washing with PBS, appropriate secondary antibodies [Donkey antirabbit Alexa Fluor 594 (#A-21207; Thermofisher Scientific) and donkey antimouse Alexa Fluor 488 (#A-21202; Thermofisher Scientific)] were added for 1 hour at RT, followed by washing. Finally, the slides were mounted with ProLongTM Gold Antifade Mountant with DAPI (P36931; Thermofisher Scientific). Images were obtained using determined confocal microscopy (Leica SP8). Average corrected total fluorescence was calculated per image for GFAP and aSyn stainings, with a mean value calculated per animal. For Zonula occludens protein 1 (ZO-1) staining, a minimum of 15 images of the epithelial lining and crypts were taken per sample. Images were then scored using a 4-point scale, with 0 = no ZO-1 staining and 3 = continuous ZO-1 staining. This scoring was done for a minimum of 20 individual epithelial lining and crypt sites, with an average score being assigned to each individual animal. All images were obtained and scored in a blinded manner.

2.6. Western blot

The brain, ileum, and colon samples were lysed in 5x vol of Na-K-Phosphate buffer (pH 7.0) by using a mechanical homogenizer. The lysates were then sonicated and centrifuged at 13,300 rpm at +4 °C for 15 minutes. The supernatants were collected, and the protein amounts were measured with the BCA method (ThermoFisher Scientific). Equal amounts of protein (~30 μg) were separated by 12% Mini-Protein TGX gels (#4568044; Bio-Rad, Hercules, CA, USA) and then transferred onto Trans-Blot Turbo Midi PVDF (#1704157; Bio-Rad) membranes by using Trans-Blot Turbo Transfer System (#1704150; Bio-Rad). The membranes were blocked with the blocking buffer [5% (W/V) skimmed milk (Valio, Helsinki, Finland), Tris-buffered saline-0.05% Tween 20 (TBS-T)] at room temperature for 1 hour and incubated overnight with primary antibodies at 4 °C. A detailed list of primary antibodies and their respective concentrations is presented in Table 1. The antibody specification was verified by their vendor, and we also verified that the antibodies produced a band with the correct molecular weight. After washing with TBS-T 3 times, the membranes were incubated with the appropriate horseradish peroxidase (HRP)-conjugated secondary antibodies for 2 hours at room temperature, goat antirabbit HRP (#31460; ThermoFisher Scientific), and goat antimouse HRP (#31430; ThermoFisher Scientific). The membranes were incubated with SuperSignal West Pico Plus Chemiluminescent Substrate (#34580; ThermoFisher Scientific) or SuperSignal West Femto Maximum Sensitivity Substrate (#34095; ThermoFisher Scientific).

Table 1
Details of antibodies used in immunohistochemistry (IHC) and western blotting (WB)

Antibody	Application	Species	Manufacturer	Product#	Dilution
GFAP	IHC	Rabbit	Dako	Z0334	1/1000
α-Synuclein	IHC	Mouse	Sigma-Aldrich	36-008	1/1000
ZO-1	IHC	Rabbit	Abcam	ab59720	1/1000
GFAP	WB	Rabbit	Abcam	ab7260	1/10000
Iba1	WB	Rabbit	Abcam	ab178846	1/1000
α-Synuclein	WB	Rabbit	Abcam	ab212184	1/1000
pS129 α-Synuclein	WB	Rabbit	Abcam	ab51253	1/1000
Tyrosine hydroxylase	WB	Mouse	Sigma-Aldrich	MAB318	1/1000
Vinculin	WB	Rabbit	Abcam	ab129002	1/10000

Immunoreactivity was visualized by the ImageQuant RT ECL Imager (GE Healthcare), and the relative optical densities of the bands were analyzed with image analysis software Image J (version 1.8.0; National Institutes of Health, Bethesda, MD, USA).

2.7. Statistical analysis

Results are expressed as mean ± SEM. Statistical analyses were performed using GraphPad Prism 5.03 software (GraphPad Software Inc., San Diego, CA, USA). Data were tested with a 1- or 2-way analysis of variance (ANOVA) followed by Tukey's multiple or Bonferroni's comparison test, respectively. The criterion for statistical significance was set at $p < 0.05$.

3. Results

3.1. Behavioral studies

The effects of the partial striatal lesion and the full MFB lesion on forelimb use were investigated 4 weeks after the surgery. The MFB lesion significantly impaired the use of the contralateral forelimb compared to the sham-lesioned animals, as indicated by the increased ipsilateral limb use preference in each test (Fig. 1; cylinder (A) and vibrissae tests (D), $p < 0.01$; adjusting steps (B) and movement initiation tests (C), $p < 0.001$ vs. sham). The overall ipsilateral limb use score (the average of 4 separate tests) revealed a clear impairment (Fig. 1E; $p < 0.001$ vs. sham) in the use of the forelimb in the MFB-lesioned rats; the average score was 0.55 ± 0.08, whereas the sham-lesioned animals showed no preference in their forelimb use (Fig. 1E; ipsilateral score −0.01 ± 0.017). The partially lesioned rats (STR group) showed a tendency to prefer the ipsilateral forelimb in each of the tests, but there were no statistically significant differences in comparison to the sham-lesioned animals. However, the combined overall ipsilateral score revealed a significant difference compared to the sham group (0.14 ± 0.11 in STR vs. −0.01 ± 0.017 in sham, $p < 0.05$).

3.2. Immunohistochemistry

Immunohistochemical analysis of the ileum and colon of the animals revealed increased levels of GFAP in both the partial STR and full MFB lesion groups. Specifically, quantification of staining in the ileum showed that the partial 6-OHDA lesion significantly increased the GFAP expression by approximately 2-fold compared to the sham-lesioned animals (4.58 ± 0.47 in the sham group vs. 8.95 ± 0.82 in the STR group, $p < 0.05$) (Fig. 1A and E). In rats subjected to the full MFB lesion, there was an even larger increase (2.3x vs. sham group) in GFAP expression (10.86 ± 1.26 in the MFB group, $p < 0.01$ vs. sham group). In the colon, the GFAP expression had been upregulated approximately 4-fold after both 6-OHDA lesion protocols, however, with no differences between the partial STR and full MFB lesion groups (6.58 ± 0.57 in the sham group vs. 24.62 ± 1.25 in the STR group vs. 23.50 ± 2.32 in the MFB group, sham vs. STR lesion and sham vs. MFB lesion $p < 0.0001$, and STR lesion vs. full lesion $p = 0.886$) (Fig. 2C and F). Neither of the 6-OHDA lesions altered the intensity of aSyn expression in the ileum (Fig. 2B and E). Instead, immunostaining of aSyn in the colon of full MFB-lesioned rats revealed a statistically significant 7-fold increase (1.52 ± 0.35 in the sham group vs. 10.32 ± 1.18 in the MFB group, $p < 0.0001$) but not in animals with the partial STR lesion (1.52 ± 0.35 vs. 4.52 ± 0.40, $p = 0.0926$) compared to sham-treated animals (Fig. 2D and F). The presence of aSyn in the colon was significantly higher in MFB-lesioned animals (by 128%) than in partially lesioned animals (4.52 ± 0.40 in the STR group vs. 10.32 ± 1.18 in the MFB group, $p = 0.0003$) (Fig. 2D and F).

No significant alteration in the ZO-1 integrity score was detected in the ileum of 6-OHDA-lesioned animals (Fig. 3A and C). Instead, in the colon, the ZO-1 barrier integrity score was significantly decreased in those animals that had undergone the 6-OHDA lesioning compared to the sham-operated controls (Fig. 3B and D). Specifically, the partial STR lesion decreased the integrity score by 0.99 points (2.50 ± 0.07 vs. 1.51 ± 0.17 sham vs. STR, $p = 0.002$), while the full lesion reduced the integrity score by 1.09 points (2.50 ± 0.07 vs. 1.41 ± 0.14 sham vs. MFB, $p = 0.0009$) in the colon.

3.3. Western blot

To validate further the results of the immunohistochemical staining in the colon and ileum, western blots were run to detect aSyn, pS129 aSyn, and GFAP levels in the intestinal samples but also in the lesioned and intact striatum. The full MFB lesion evoked by 6-OHDA significantly increased the total aSyn levels in the colon and also elevated the pS129 aSyn and GFAP levels in the colon (Fig. 4A and B). Interestingly, the partial STR lesion decreased the total aSyn levels in comparison to the sham-lesioned animals and did not increase pS129 aSyn or GFAP protein expression (Fig. 4C). The same proteins were detected also in the ileum, but no changes between the treatment groups were evident (Fig. 4D–F).

In the striatum, the 6-OHDA injected side of the brain showed elevated levels of pS129 aSyn and total aSyn (Fig. 5A and B), and particularly, the MFB lesion increased the levels of both aSyn markers. However, the GFAP levels were most significantly elevated in

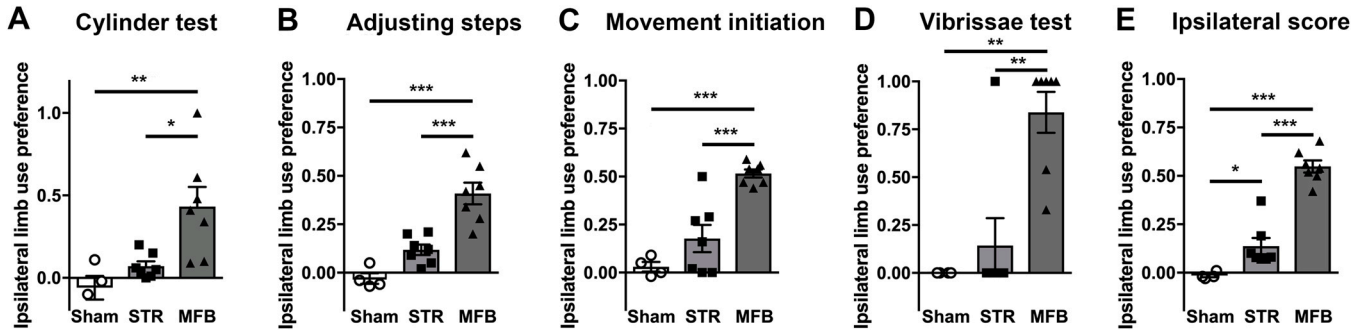

Fig. 1. The behavioral characterization of different lesion protocols at 4 weeks after the 6-OHDA injections. The following tests were performed: Cylinder test (A), adjusting steps (B), movement initiation (C), vibrissae test (D), and ipsilateral scoring (E). The bars represent the preference to use the forelimb ipsilateral to the lesion. A high ipsilateral preference indicates a dysfunctional use of the contralateral limb and more severe unilateral nigrostriatal dopaminergic damage. The ipsilateral score is calculated as an average of 4 individual tests for each animal. All results are shown as mean ± SEM. * = $p < 0.05$, ** = $p < 0.01$, *** = $p < 0.001$, and **** = $p < 0.0001$. One-way ANOVA with Tukey's post hoc test.

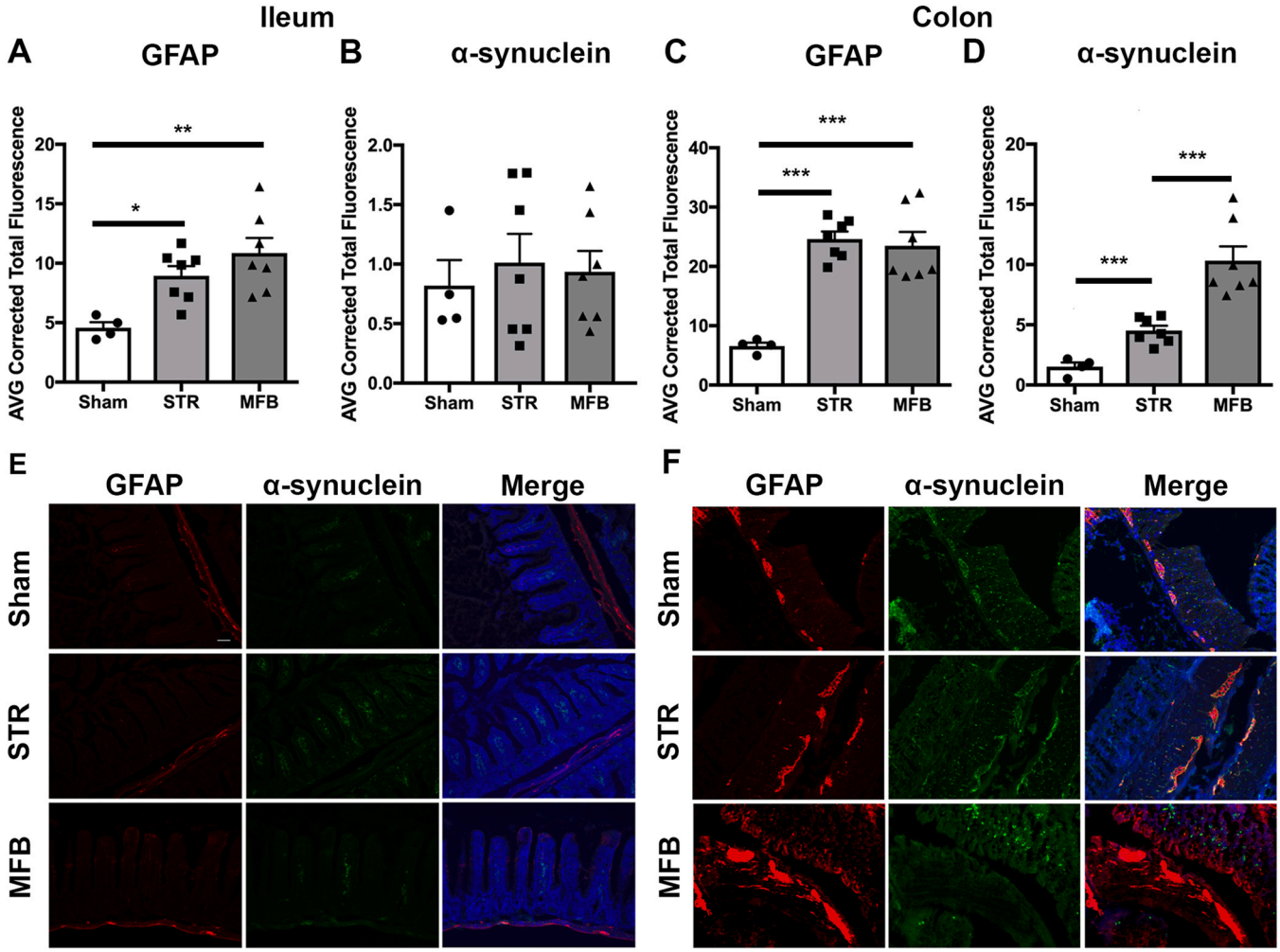

Fig. 2. Immunohistochemical analysis of GFAP and native aSyn in the ileal and colon samples. Staining of GFAP (A) and α-synuclein (B) in the ileum; staining of GFAP (C) and α-synuclein (D) in the colon. Representative immunohistochemical staining images of ileum (E) and colon (F) samples. GFAP expression (red) as a marker for enteric glial cells, α-synuclein expression (green), and DAPI staining (blue) (scale bar: 50 µm). All results are shown as mean ± SEM. $^{*}=p<0.05$, $^{**}=p<0.01$, $^{***}=p<0.001$, and $^{****}=p<0.0001$, 1-way ANOVA with Tukey's post hoc test.

the partial STR lesion group, but the ionized calcium-binding adapter molecule 1 (Iba1) was significantly elevated on the injected side (Fig. 5C and D). As expected, tyrosine hydroxylase (TH) expression was significantly decreased in the ipsilateral compared to the contralateral striatum after the full MFB lesion ($p < 0.0001$). Instead, the partial STR lesion did not significantly reduce TH expression between the striata ($p = 0.557$). Notably, even the sham injection with the vehicle introduced some variation in the TH expression between the intact and lesioned striatum (Fig. 5E).

4. Discussion

As far as we are aware, this is the first study to demonstrate that a commonly used toxin model of PD, 6-OHDA, elevates the intensity of aSyn expression and phosphorylation in the rat colon. The earlier assumption has been that 6-OHDA induces strong oxidative stress, mitochondrial dysfunction, and local neuroinflammation, leading to neuronal death (El-Gamal et al., 2021). However, although aSyn increases the toxicity of 6-OHDA (Alvarez-Fischer et al., 2008) and 6-OHDA induces aSyn expression in the SN (Wang et al., 2021), in the rodent brain, this does not lead to any aSyn aggregation and the presence of Lewy body-like structures. Furthermore, the effects of nigral or striatal 6-OHDA injection are on gastrointestinal functionality, and while certain pathological markers have been examined previously, this is the first study to show that 6-OHDA-induced brain lesions elevate aSyn and Ser129 phosphorylated aSyn levels in the colon. Notably, it has been shown earlier that intrastriatal administration of rotenone, another dopamine-specific neurotoxin, also induced aSyn accumulation in the colon (Perez-Pardo et al., 2018), suggesting that the alterations in the colon aSyn levels are not 6-OHDA specific but are rather associated with nigrostriatal dopaminergic damage.

Here, we utilized 2 validated unilateral 6-OHDA lesion models, that is, a full MFB model producing a nearly complete loss of dopamine in the lesioned side striatum (Leikas et al., 2017) and a partial striatal lesion, which has been shown to induce an approximately 50% dopamine depletion in the ipsilateral striatum at 5 weeks after the toxin administration (Zhurakovskaya et al., 2019). These 2 models have rather different outcomes at both the behavioral and biochemical levels; the partial striatal lesion produces much milder behavioral effects that were also evident in our sensorimotor test battery. By performing a series of simple sensorimotor tests and calculating a combined score covering multiple domains of sensorimotor functions, we have previously shown that it is possible to detect even as little as a 50% unilateral dopamine depletion in the striatum (Leikas et al., 2017). The significantly

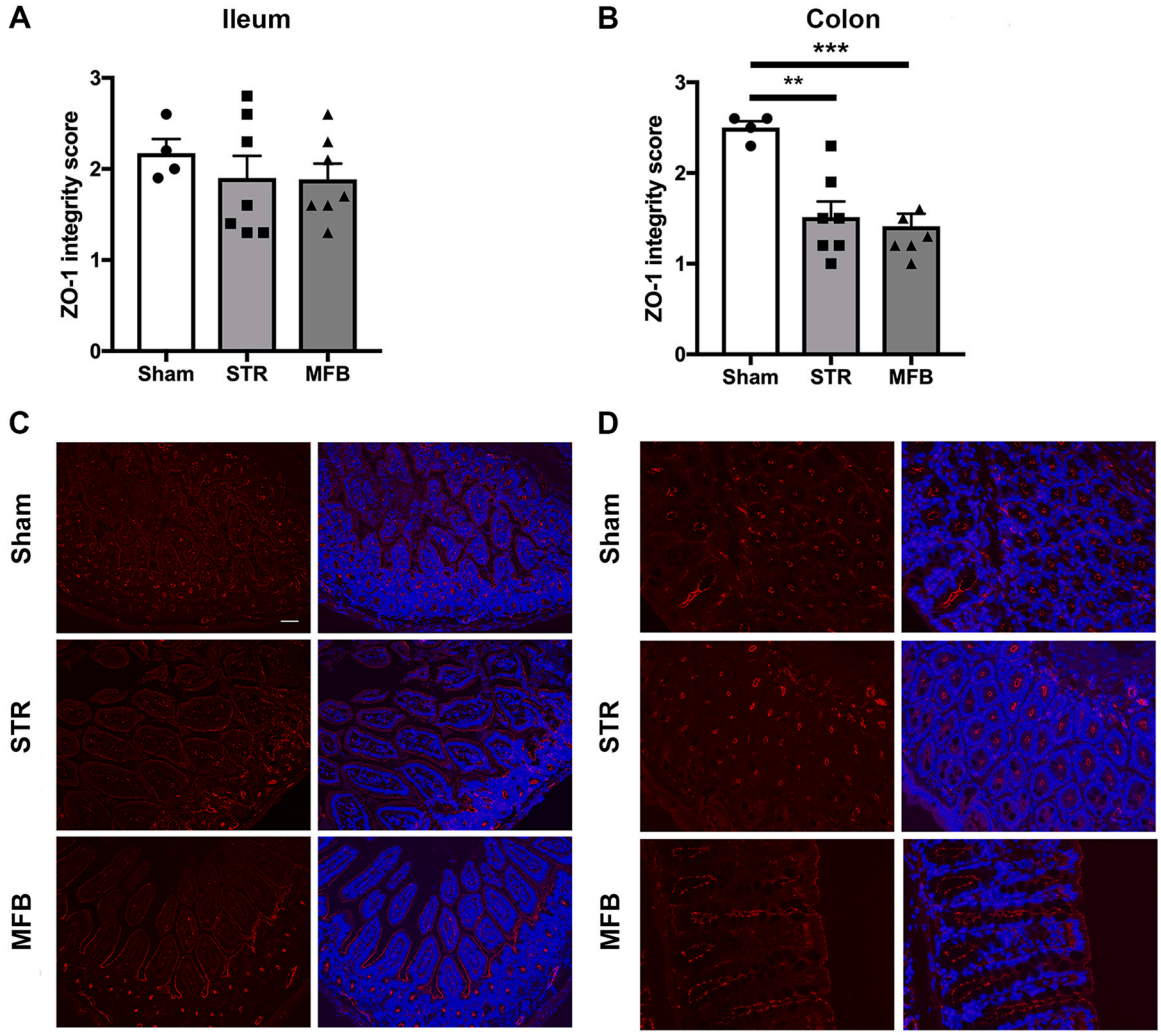

Fig. 3. Immunohistochemical analysis of ZO-1 expression levels in rat intestinal samples. Scoring of ZO-1 staining in ileum (A) and colon (B). Representative immunohistochemical staining images of ileum (C) and colon (D) samples. ZO-1 expression (red) and DAPI staining (blue) (scale bar: 50 μm). All results are shown as mean ± SEM. $^{*}p < 0.05$, $^{**}p < 0.01$, $^{***}p < 0.001$, and $^{****}p < 0.0001$, 1-way ANOVA with Tukey's post hoc test.

elevated combined ipsilateral score and the observed trend toward decreased striatal TH expression in partially lesioned rats confirm that the striatal 6-OHDA injection had produced a marked dopaminergic dysfunction in the ipsilateral striatum. The full MFB lesion, on the other hand, evoked a significant ipsilateral limb use preference in all behavioral tests, indicating severe unilateral dopaminergic dysfunction in the striatum. The behavioral findings in MFB rats were further validated with TH expression data showing a significant loss of TH expression in the striatum ipsilateral to the lesion. These results underline the different natures of these 2 models: the partial striatal model mimics early-stage PD and is best utilized in experiments assessing the efficacy of disease-modifying treatments, whereas the full MFB model reflects the situation in patients with advanced or late-stage PD.

Constipation is a common symptom in PD, and it has even been considered an early symptom preceding the motor symptoms [for a review, see (O'Day C et al., 2022)]. The first hypothesis proposed that neuronal degeneration also occurs in neurons of the enteric nervous system. In the colon, a reduced number of submucosal neurons have been detected in PD patients (Lebouvier et al., 2010), but this has not been seen in the small intestine, which includes the ileum (O'Day C et al., 2022). In the current study, we also observed significant changes in the colon but not in the ileum, suggesting that the brain-induced changes in PD are more pronounced in the colon. In addition, recent studies showing that the fecal microbiome is altered in PD patients further promote the role of the gut–brain axis in PD (Boertien et al., 2022; Scheperjans et al., 2015; Takahashi et al., 2022). This has led to the hypothesis that there are 2 forms of PD—a "gut-first" and a "brain-first" PD—and there is some evidence from clinical imaging, as well as from neuropathological stainings, supporting this model (Borghammer et al., 2021; Horsager et al., 2020). The gut-first model suggests that pathogenic aSyn originates in the enteric or peripheral nervous system, spreads from the gut via the vagus nerve to the dorsal motor nucleus of the vagus, and thereafter reaches theSN. In addition, aSyn can spread from the gut to the locus coeruleus via a bidirectional sympathetic route and further propagate to the SN (Van Den Berge et al., 2019). In the brain-first model, the aSyn pathology originates in the central nervous system (CNS), particularly in the amygdala, SN, and locus coeruleus, and spreads through the sympathetic route to the peripheral nervous system (Borghammer et al., 2022).

Despite being one of the most widely used PD models, the effect of 6-OHDA on the gut–brain axis has not been extensively studied. Constipation and defecatory dysfunctions are well documented in various 6-OHDA models. Blandini et al. (2009) reported that, after a unilateral MFB lesion, fecal daily output reduced starting from day

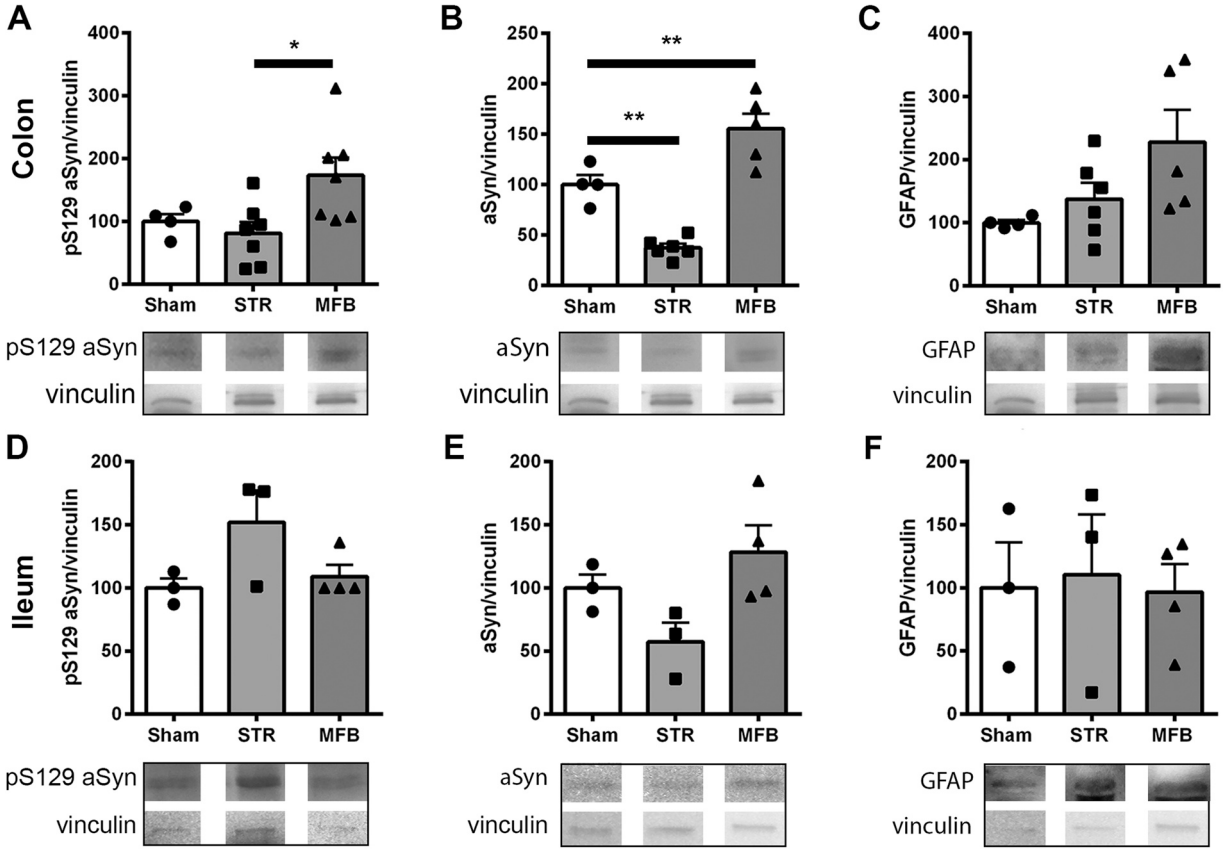

Fig. 4. 6-OHDA lesion to medial forebrain bundle (MFB)-induced Ser129 phosphorylated (pS129) aSyn protein expression in the western blot in colon samples (A). A similar effect was seen in total aSyn levels after MFB lesion, but striatal lesion (STR) reduced only total aSyn levels (B). GFAP was also increased but not significantly (C). In ileum samples (D), (E), and (F), no significant changes were detected. Data are presented as mean ± SEM. * = $p < 0.05$, ** $p < 0.01$, 1-way ANOVA with Tukey's post hoc test.

14 after the lesion, but no changes were observed in the number of myenteric neurons in the colon. Rats with a complete unilateral loss of striatal dopamine induced by a nigrostriatal 6-OHDA lesion showed decreased colonic transit rate (Fornai et al., 2016). Furthermore, rats with a bilateral partial 6-OHDA lesion showed reduced fecal water content and outlet obstruction constipation, as evidenced by a delayed transit time, increased contractive tension, and fecal retention in the colorectum (Zhang et al., 2021). Other studies using unilateral MFB or SNpc-targeted lesions by 6-OHDA showed that dopamine D2 receptors and peristaltic reflexes were significantly decreased in the colon at four weeks post-lesion (Colucci et al., 2012; Toti and Travagli, 2014). Similar findings were seen 6 weeks after bilateral injection of 6-OHDA to the substantia nigra pars compacta, where decreased levels of both D1 and D2 receptors and increased levels of oxidative stress markers were seen in the colon (Garrido-Gil et al., 2018). However, these investigators did not report if there were changes in inflammatory markers, but Thomasi et al. (2022) and Pellegrini et al. (2016) did claim that a unilateral striatal 6-OHDA injection elevated Iba1 and GFAP immunoreactivity, particularly in the early stage, but a long-term elevation in GFAP was seen as well. In the current study, we demonstrated that GFAP-immunoreactivity was elevated particularly in the colon after a striatal 6-OHDA lesion at 5 weeks postlesion, but a significant increase was also seen in the immunoreactive GFAP in the ileum. This finding was further supported by the western blotting analysis, where a (non-significant) trend toward elevated GFAP levels in the colon was observed after both lesions, but the increase was more pronounced in rats with the full MFB lesion. This suggests that the degree of nigrostriatal dopaminergic neuron degeneration correlates with the level of enteric glial cell activation in the current model.

Elevated GFAP mRNA expression levels in the colon have also been detected in PD patients, and they correlate with the colonic expression of proinflammatory cytokines (Clairembault et al., 2014; Devos et al., 2013). There are several reports that, particularly, the presence of irritable bowel syndrome, where an intestinal infection is present (Ng et al., 2018), increases the risk for PD [for a meta-analysis, see Fu et al. (2020)]. Moreover, there are several shared genetic loci between PD, Crohn's disease, and ulcerative colitis; the latter 2 diseases are associated with inflammation in the intestinal tract (Witoelar et al., 2017). Enteric GFAP-positive glial cells are present in myenteric and submucosal ganglia, and are known to regulate the intestinal immune system and epithelial barrier function (Grundmann et al., 2019). However, it is not known why the enteric glial cells become activated in PD or in the 6-OHDA lesion model. One possibility is that centrally administered 6-OHDA can access the enteric nervous system via the vagus nerve, but, since 6-OHDA is rapidly auto-oxidized (Varešlija et al., 2020), this seems unlikely. However, it is possible that the proinflammatory cytokines secreted by glial cells induce enteric glial cell activation via the vagus nerve. We also found changes in ZO-1, a tight junction marker, indicating that the 6-OHDA lesion had damaged the colon's epithelial layer. Abnormalities in the colon wall have been observed in PD patients, with decreased levels of occludin, another tight junction marker, but the levels of ZO-1 were normal (Clairembault et al., 2015). It has been suggested that a "leaky gut" can evoke inflammation and trigger GFAP expression via increased bacterial leakage and an immune reaction on the colon wall. However, we cannot conclude if the increase in GFAP causes a decrease in ZO-1 or vice versa. Another option is that the intense production of reactive oxygen species by 6-OHDA may act as a trigger for GFAP activation

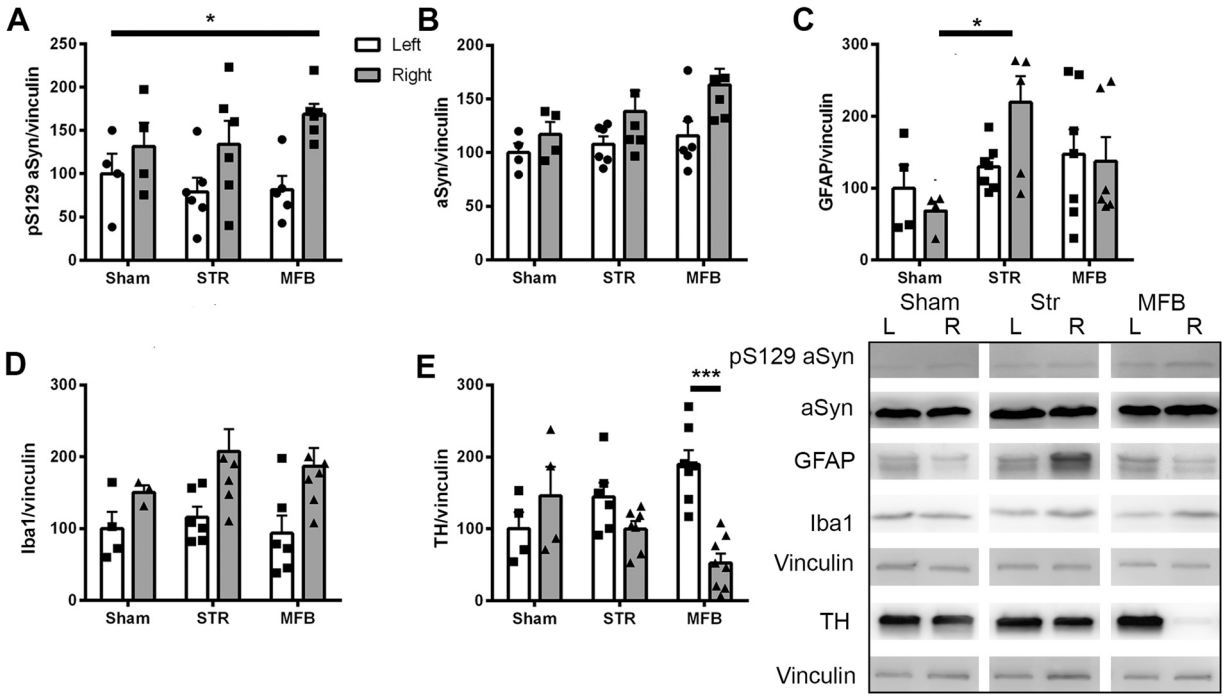

Fig. 5. Both striatal (STR) and medial forebrain bundle (MFB) 6-OHDA lesions generally induced elevated expression levels of Ser129 phosphorylated aSyn (pS129 aSyn) in the lesioned side (right) (A; $p < 0.0022$ left vs. right striatum; 2-way ANOVA) with the same effect being seen in total aSyn levels (B; $p < 0.023$ left vs. right striatum, 2-way ANOVA). The GFAP expression was significantly increased only in the STR lesion group (C), but the amounts of the other glial cell marker, Iba1, were elevated on the lesioned side (D; $p < 0.0015$ left vs. right striatum, 2-way ANOVA). Tyrosine hydroxylase (TH) levels were significantly decreased in the MFB lesion as expected (E; $p < 0.0105$ left vs. right striatum, 2-way ANOVA). $^{*}p < 0.05$, $^{***}p < 0.001$, 2-way ANOVA with Bonferroni's post hoc test.

and epithelial cell damage. Although there are no reports about these phenomena, oxidative stress and reactive oxygen species production in the vagus nerve have been reported to induce PD-like changes in the CNS in experimental models, including aSyn aggregation and propagation (Musgrove et al., 2019).

The most novel finding in the study was the increase of aSyn levels and Ser129 phosphorylation in the colon after the full MFB lesion, and there seemed to be even a clear correlation between the aSyn levels and the severity of the lesion. Ser129 phosphorylated aSyn is the dominant form of aSyn in Lewy bodies, and although phosphorylation can target misfolded aSyn to degradation, it also increases aSyn instability and induces its aggregation [for a review, see Manzanza et al. (2021)]. After Braak et al. (2003) proposed the hypothesis of toxic aSyn propagation, the role of aSyn in the gut–-brain axis has been intensively studied, particularly the movement of aSyn from the gut to the brain. This phenomenon has been shown in experimental models (Challis et al., 2020; Holmqvist et al., 2014; Kim et al., 2019; Van Den Berge et al., 2019, 2021), and aggregated aSyn and Lewy bodies, as well as Ser129 phosphorylated aSyn, have been detected in the vagus nerve (Gelpi et al., 2014; Wakabayashi et al., 1999) and the enteric nervous system (Braak et al., 2006) of PD patients. It should be noted that the patient samples were obtained from patients already diagnosed with PD, making it difficult to draw conclusions about at what stage of the disease, the aSyn aggregation in the enteric nervous system and vagus nerve had occurred. On the other hand, a recent study in nonhuman primates challenged the role of the vagus nerve and proposed that blood circulation could act as a route for bidirectional aSyn transport between the enteric nervous system and the brain (Arotcarena et al., 2020). Our results support the theory that there is a bidirectional connection between brain and gut, and suggest that a pathological event in the brain with DAergic cell degeneration and inflammation, even without significant aSyn aggregation, can elevate aSyn levels and phosphorylation, as well as inflammatory markers in the colon. The limitation of the current study is that we did not analyze the aggregated forms of aSyn or examine the vagus nerve at different time points to detect the temporal changes and origins of aSyn or GFAP.

One of the major questions is how the injection of 6-OHDA into the brain can induce particularly aSyn levels in the colon. If 6-OHDA-induced oxidative stress is present in the colon, it can also act as a trigger for aSyn aggregation [for a review, see Abramov et al. (2020)]. The elevated GFAP levels suggest that an inflammatory process is present in the colon, and inflammation has been shown to induce Ser129 aSyn phosphorylation in preclinical settings (Reimer et al., 2018). However, there is also convincing evidence that aSyn aggregates can induce glial cell activation [for a review, see Chavarría et al. (2022)], but, in the current study, we did not investigate aSyn aggregation in these cells. The data suggest that 6-OHDA-induced GFAP activation, either before or after the increases in colon permeability, resulted in elevated aSyn levels and phosphorylation, emphasizing the role of inflammation in these aSyn-changes. Recent findings of aSyn-reactive T-cells with the highest reactivity before and at the time of PD diagnosis support this proposal, indicating that inflammation in PD occurs before the development of motor symptoms (Lindestam Arlehamn et al., 2020; Sulzer et al., 2017).

In conclusion, the present study demonstrates that intracerebral 6-OHDA administration leads to gastrointestinal abnormalities, including aSyn accumulation, glial cell activation, and increased intestinal permeability. These findings support the theory that the gut–brain axis interactions in PD are bidirectional, and the detrimental process may also start in the brain and subsequently become evident in the gut. This certainly warrants further studies in PD

patients, and while it would be particularly important to study individuals before the motor symptoms occur and the diagnosis has been confirmed, this will require the development of better biomarkers for early PD. Our results also validate the use of 6-OHDA as an experimental model for investigating the enteric nervous system and gut–brain axis changes in PD.

CRediT authorship contribution statement

Henjing Cui: Investigation, Methodology, Formal analysis, and Writing—original draft; **Joshua Elford**: Investigation, Methodology, Formal analysis, Visualization, and Writing—original draft; **Okko Alitalo**: Investigation and Formal analysis; **Paula Perez-Pardo**: Investigation, Methodology, Formal analysis, Visualization, Writing—original draft, and Writing—review and editing; **Janne Tampio**: Investigation, Methodology, Formal analysis, and Writing—review and editing; **Kristiina Huttunen**: Conceptualization, Resources, and Writing—review and editing; **Aletta Kraneveld**: Conceptualization, Resources, and Writing—review and editing; **Markus Forsberg**: Conceptualization, Resources, Project administration, Writing—original draft, and Writing—review and editing; **Timo Myöhänen**: Investigation, Methodology, Resources, Funding, Formal analysis, Visualization, Writing—original draft, and Writing—review and editing; and **Aaro Jalkanen**: Investigation, Methodology, Formal analysis, Funding, Visualization, Writing—original draft, and Writing—review and editing.

Disclosure statement

The authors declare no conflicts of interest.

Acknowledgements

This study was financially supported by the School of Pharmacy, University of Eastern Finland (NFG grant for AJJ), and by Sigrid Jusélius Foundation (for TTM). The funding source had no role in the study design; in the collection, analysis, and interpretation of data; in the writing of the report; and in the decision to submit the article for publication. Dr. Ewen MacDonald is acknowledged for revising the language of the manuscript.

References

Abramov, A.Y., Potapova, E.V., Dremin, V.V., Dunaev, A.V., 2020. Interaction of oxidative stress and misfolded proteins in the mechanism of neurodegeneration. Life 10, 101. https://doi.org/10.3390/life10070101

Alvarez-Fischer, D., Henze, C., Strenzke, C., Westrich, J., Ferger, B., Höglinger, G.U., Oertel, W.H., Hartmann, A., 2008. Characterization of the striatal 6-OHDA model of Parkinson's disease in wild type and alpha-synuclein-deleted mice. Exp. Neurol. 210, 182–193. https://doi.org/10.1016/j.expneurol.2007.10.012

Antunes, L., Frasquilho, S., Ostaszewski, M., Weber, J., Longhino, L., Antony, P., Baumuratov, A., Buttini, M., Shannon, K.M., Balling, R., Diederich, N.J., 2016. Similar α-Synuclein staining in the colon mucosa in patients with Parkinson's disease and controls. Mov. Disord. Off. J. Mov. Disord. Soc. 31, 1567–1570. https://doi.org/10.1002/mds.26702

Arotcarena, M.L., Dovero, S., Prigent, A., Bourdenx, M., Camus, S., Porras, G., Thiolat, M.L., Tasselli, M., Aubert, P., Kruse, N., Mollenhauer, B., Trigo Damas, I., Estrada, C., Garcia-Carrillo, N., Vaikath, N.N., El-Agnaf, O.M.A., Herrero, M.T., Vila, M., Obeso, J.A., Derkinderen, P., B., Dehay, Bezard, E., 2020. Bidirectional gut-to-brain and brain-to-gut propagation of synucleinopathy in non-human primates. Brain 143, 1462–1475. https://doi.org/10.1093/brain/awaa096

Blandini, F., Balestra, B., Levandis, G., Cervio, M., Greco, R., Tassorelli, C., Colucci, M., Faniglione, M., Bazzini, E., Nappi, G., Clavenzani, P., Vigneri, S., De Giorgio, R., Tonini, M., 2009. Functional and neurochemical changes of the gastrointestinal tract in a rodent model of Parkinson's disease. Neurosci. Lett. 467, 203–207. https://doi.org/10.1016/j.neulet.2009.10.035

Boertien, J.M., Murtomäki, K., Pereira, P.A.B., van der Zee, S., Mertsalmi, T.H., Levo, R., Nojonen, T., Mäkinen, E., Jaakkola, E., Laine, P., Paulin, L., Pekkonen, E., Kaasinen, V., Auvinen, P., Scheperjans, F., van Laar, T., PPNN Study Group,, 2022. Fecal microbiome alterations in treatment-naive de novo Parkinson's disease. NPJ Parkinsons Dis. 8, 129. https://doi.org/10.1038/s41531-022-00395-8

Borghammer, P., Horsager, J., Andersen, K., Van Den Berge, N., Raunio, A., Murayama, S., Parkkinen, L., Myllykangas, L., 2021. Neuropathological evidence of body-first vs. brain-first Lewy body disease. Neurobiol. Dis. 161, 105557. https://doi.org/10.1016/j.nbd.2021.105557

Borghammer, P., Just, M.K., Horsager, J., Skjærbæk, C., Raunio, A., Kok, E.H., Savola, S., Murayama, S., Saito, Y., Myllykangas, L., Van Den Berge, N., 2022. A postmortem study suggests a revision of the dual-hit hypothesis of Parkinson's disease. NPJ Parkinsons Dis. 8, 166. https://doi.org/10.1038/s41531-022-00436-2

Braak, H., de Vos, R.A.I., Bohl, J., Del Tredici, K., 2006. Gastric α-synuclein immunoreactive inclusions in Meissner's and Auerbach's plexuses in cases staged for Parkinson's disease-related brain pathology. Neurosci. Lett. 396, 67–72. https://doi.org/10.1016/j.neulet.2005.11.012

Braak, H., Del Tredici, K., Rüb, U., de Vos, R.A.I., Jansen Steur, E.N.H., Braak, E., 2003. Staging of brain pathology related to sporadic Parkinson's disease. Neurobiol. Aging 24, 197–211. https://doi.org/10.1016/s0197-4580(02)00065-9

Challis, C., Hori, A., Sampson, T.R., Yoo, B.B., Challis, R.C., Hamilton, A.M., Mazmanian, S.K., Volpicelli-Daley, L.A., Gradinaru, V., 2020. Gut-seeded α-synuclein fibrils promote gut dysfunction and brain pathology specifically in aged mice. Nat. Neurosci. 23, 327–336. https://doi.org/10.1038/s41593-020-0589-7

Chavarría, C., Ivagnes, R., Souza, J.M., 2022. Extracellular alpha-synuclein: mechanisms for glial cell internalization and activation. Biomolecules 12, 655. https://doi.org/10.3390/biom12050655

Clairembault, T., Kamphuis, W., Leclair-Visonneau, L., Rolli-Derkinderen, M., Coron, E., Neunlist, M., Hol, E.M., Derkinderen, P., 2014. Enteric GFAP expression and phosphorylation in Parkinson's disease. J. Neurochem. 130, 805–815. https://doi.org/10.1111/jnc.12742

Clairembault, T., Leclair-Visonneau, L., Coron, E., Bourreille, A., Le Dily, S., Vavasseur, F., Heymann, M.-F., Neunlist, M., Derkinderen, P., 2015. Structural alterations of the intestinal epithelial barrier in Parkinson's disease. Acta Neuropathol. Commun. 3, 12. https://doi.org/10.1186/s40478-015-0196-0

Colucci, M., Cervio, M., Faniglione, M., Angelis, S.D., Pajoro, M., Levandis, G., Tassorelli, C., Blandini, F., Feletti, F., Giorgio, R.D., Dellabianca, A., Tonini, S., Tonini, M., 2012. Intestinal dysmotility and enteric neurochemical changes in a Parkinson's disease rat model. Auton. Neurosci. Basic Clin. 169, 77–86. https://doi.org/10.1016/j.autneu.2012.04.005

Devos, D., Lebouvier, T., Lardeux, B., Biraud, M., Rouaud, T., Pouclet, H., Coron, E., Bruley des Varannes, S., Naveilhan, P., Nguyen, J.-M., Neunlist, M., Derkinderen, P., 2013. Colonic inflammation in Parkinson's disease. Neurobiol. Dis. 50, 42–48. https://doi.org/10.1016/j.nbd.2012.09.007

Dodiya, H.B., Forsyth, C.B., Voigt, R.M., Engen, P.A., Patel, J., Shaikh, M., Green, S.J., Naqib, A., Roy, A., Kordower, J.H., Pahan, K., Shannon, K.M., Keshavarzian, A., 2020. Chronic stress-induced gut dysfunction exacerbates Parkinson's disease phenotype and pathology in a rotenone-induced mouse model of Parkinson's disease. Neurobiol. Dis. 135, 104352. https://doi.org/10.1016/j.nbd.2018.12.012

El-Gamal, M., Salama, M., Collins-Praino, L.E., Baetu, I., Fathalla, A.M., Soliman, A.M., Mohamed, W., Moustafa, A.A., 2021. Neurotoxin-induced rodent models of Parkinson's disease: benefits and drawbacks. Neurotox. Res. 39, 897–923. https://doi.org/10.1007/s12640-021-00356-8

Fornai, M., Pellegrini, C., Antonioli, L., Segnani, C., Ippolito, C., Barocelli, E., Ballabeni, V., Vegezzi, G., Harraq, Z.A., Blandini, F., Levandis, G., Cerri, S., Blandizzi, C., Bernardini, N., Colucci, R., 2016. Enteric dysfunctions in experimental Parkinson's disease: alterations of excitatory cholinergic neurotransmission regulating colonic motility in rats. J. Pharmacol. Exp. Ther. 356, 434–444. https://doi.org/10.1124/jpet.115.228510

Fu, P., Gao, M., Yung, K.K.L., 2020. Association of intestinal disorders with Parkinson's disease and Alzheimer's disease: a systematic review and meta-analysis. ACS Chem. Neurosci. 11, 395–405. https://doi.org/10.1021/acschemneuro.9b00607

Garrido-Gil, P., Rodriguez-Perez, A.I., Dominguez-Meijide, A., Guerra, M.J., Labandeira-Garcia, J.L., 2018. Bidirectional neural interaction between central dopaminergic and gut lesions in Parkinson's disease models. Mol. Neurobiol. 55, 7297–7316. https://doi.org/10.1007/s12035-018-0937-8

Gelpi, E., Navarro-Otano, J., Tolosa, E., Gaig, C., Compta, Y., Rey, M.J., Martí, M.J., Hernández, I., Valldeoriola, F., Reñé, R., Ribalta, T., 2014. Multiple organ involvement by alpha-synuclein pathology in Lewy body disorders. Mov. Disord. 29, 1010–1018. https://doi.org/10.1002/mds.25776

Grundmann, D., Loris, E., Maas-Omlor, S., Huang, W., Scheller, A., Kirchhoff, F., Schäfer, K.-H., 2019. Enteric glia: S100, GFAP, and beyond. Anat. Rec. 302, 1333–1344. https://doi.org/10.1002/ar.24128

Holmqvist, S., Chutna, O., Bousset, L., Aldrin-Kirk, P., Li, W., Björklund, T., Wang, Z.-Y., Roybon, L., Melki, R., Li, J.-Y., 2014. Direct evidence of Parkinson pathology spread from the gastrointestinal tract to the brain in rats. Acta Neuropathol. (Berl.) 128, 805–820. https://doi.org/10.1007/s00401-014-1343-6

Horsager, J., Andersen, K.B., Knudsen, K., Skjærbæk, C., Fedorova, T.D., Okkels, N., Schaeffer, E., Bonkat, S.K., Geday, J., Otto, M., Sommerauer, M., Danielsen, E.H., Bech, E., Kraft, J., Munk, O.L., Hansen, S.D., Pavese, N., Göder, R., Brooks, D.J., Berg, D., Borghammer, P., 2020. Brain-first versus body-first Parkinson's disease: a multimodal imaging case-control study. Brain J. Neurol. 143, 3077–3088. https://doi.org/10.1093/brain/awaa238

Keshavarzian, A., Green, S.J., Engen, P.A., Voigt, R.M., Naqib, A., Forsyth, C.B., Mutlu, E., Shannon, K.M., 2015. Colonic bacterial composition in Parkinson's disease. Mov. Disord. Off. J. Mov. Disord. Soc. 30, 1351–1360. https://doi.org/10.1002/mds.26307

Kim, S., Kwon, S.-H., Kam, T.-I., Panicker, N., Karuppagounder, S.S., Lee, S., Lee, J.H., Kim, W.R., Kook, M., Foss, C.A., Shen, C., Lee, H., Kulkarni, S., Pasricha, P.J., Lee, G.,

Pomper, M.G., Dawson, V.L., Dawson, T.M., Ko, H.S., 2019. Transneuronal propagation of pathologic α-synuclein from the gut to the brain models Parkinson's disease. Neuron 103, 627–641.e7. https://doi.org/10.1016/j.neuron.2019.05.035

Klingelhoefer, L., Reichmann, H., 2015. Pathogenesis of Parkinson disease—the gut-brain axis and environmental factors. Nat. Rev. Neurol. 11, 625–636. https://doi.org/10.1038/nrneurol.2015.197

Lebouvier, T., Neunlist, M., Bruley des Varannes, S., Coron, E., Drouard, A., N'Guyen, J.-M., Chaumette, T., Tasselli, M., Paillusson, S., Flamand, M., Galmiche, J.-P., Damier, P., Derkinderen, P., 2010. Colonic biopsies to assess the neuropathology of Parkinson's disease and its relationship with symptoms. PloS One 5, e12728. https://doi.org/10.1371/journal.pone.0012728

Leikas, J.V., Kääriäinen, T.M., Jalkanen, A.J., Lehtonen, M., Rantamäki, T., Forsberg, M.M., 2017. Combined ipsilateral limb use score as an index of motor deficits and neurorestoration in parkinsonian rats. J. Neurosci. Res 95, 1858–1870. https://doi.org/10.1002/jnr.24022

Li, X., Yang, W., Li, X., Chen, M., Liu, C., Li, J., Yu, S., 2020. Alpha-synuclein oligomerization and dopaminergic degeneration occur synchronously in the brain and colon of MPTP-intoxicated parkinsonian monkeys. Neurosci. Lett. 716, 134640. https://doi.org/10.1016/j.neulet.2019.134640

Lindestam Arlehamn, C.S., Dhanwani, R., Pham, J., Kuan, R., Frazier, A., Rezende Dutra, J., Phillips, E., Mallal, S., Roederer, M., Marder, K.S., Amara, A.W., Standaert, D.G., Goldman, J.G., Litvan, I., Peters, B., Sulzer, D., Sette, A., 2020. α-Synuclein-specific T cell reactivity is associated with preclinical and early Parkinson's disease. Nat. Commun. 11, 1875. https://doi.org/10.1038/s41467-020-15626-w

Liu, B., Fang, F., Pedersen, N.L., Tillander, A., Ludvigsson, J.F., Ekbom, A., Svenningsson, P., Chen, H., Wirdefeldt, K., 2017. Vagotomy and Parkinson disease: a Swedish register-based matched-cohort study. Neurology 88, 1996–2002. https://doi.org/10.1212/WNL.0000000000003961

Manzanza, N., de, O., Sedlackova, L., Kalaria, R.N., 2021. Alpha-synuclein post-translational modifications: implications for pathogenesis of Lewy body disorders. Front. Aging Neurosci. 13.

McQuade, R.M., Singleton, L.M., Wu, H., Lee, S., Constable, R., Di Natale, M., Ringuet, M.T., Berger, J.P., Kauhausen, J., Parish, C.L., Finkelstein, D.I., Furness, J.B., Diwakarla, S., 2021. The association of enteric neuropathy with gut phenotypes in acute and progressive models of Parkinson's disease. Sci. Rep. 11, 7934. https://doi.org/10.1038/s41598-021-86917-5

Mertsalmi, T.H., But, A., Pekkonen, E., Scheperjans, F., 2021. Irritable bowel syndrome and risk of Parkinson's disease in Finland: a nationwide registry-based cohort study. J. Parkinsons Dis. 11, 641–651. https://doi.org/10.3233/JPD-202330

Musgrove, R.E., Helwig, M., Bae, E.-J., Aboutalebi, H., Lee, S.-J., Ulusoy, A., Monte, D.A.D., 2019. Oxidative stress in vagal neurons promotes parkinsonian pathology and intercellular α-synuclein transfer. J. Clin. Invest. 129, 3738–3753. https://doi.org/10.1172/JCI127330

Ng, Q.X., Soh, A.Y.S., Loke, W., Lim, D.Y., Yeo, W.-S., 2018. The role of inflammation in irritable bowel syndrome (IBS). J. Inflamm. Res. 11, 345–349. https://doi.org/10.2147/JIR.S174982

O'Day, C., Finkelstein, D.I., Diwakarla, S., McQuade, R.M., 2022. A critical analysis of intestinal enteric neuron loss and constipation in Parkinson's disease. PubMed [WWW Document]. Available at: ⟨https://pubmed.ncbi.nlm.nih.gov/35848035/⟩. Accessed December 12, 2022.

Pellegrini, C., Fornai, M., Colucci, R., Tirotta, E., Blandini, F., Levandis, G., Cerri, S., Segnani, C., Ippolito, C., Bernardini, N., Cseri, K., Blandizzi, C., Haskó, G., Antonioli, L., 2016. Alteration of colonic excitatory tachykininergic motility and enteric inflammation following dopaminergic nigrostriatal neurodegeneration. J. Neuroinflammation 13, 146. https://doi.org/10.1186/s12974-016-0608-5

Pellegrini, C., D'Antongiovanni, V., Miraglia, F., Rota, L., Benvenuti, L., Di Salvo, C., Testa, G., Capsoni, S., Carta, G., Antonioli, L., Cattaneo, A., Blandizzi, C., Colla, E., Fornai, M., 2022. Enteric α-synuclein impairs intestinal epithelial barrier through caspase-1-inflammasome signaling in Parkinson's disease before brain pathology. NPJ Parkinsons Dis. 8, 9. https://doi.org/10.1038/s41531-021-00263-x

Perez-Pardo, P., Dodiya, H.B., Broersen, L.M., Douna, H., van Wijk, N., Lopes da Silva, S., Garssen, J., Keshavarzian, A., Kraneveld, A.D., 2018. Gut–brain and brain–gut axis in Parkinson's disease models: effects of a uridine and fish oil diet. Nutr. Neurosci. 21, 391–402. https://doi.org/10.1080/1028415X.2017.1294555

Perez-Pardo, P., Dodiya, H.B., Engen, P.A., Forsyth, C.B., Huschens, A.M., Shaikh, M., Voigt, R.M., Naqib, A., Green, S.J., Kordower, J.H., Shannon, K.M., Garssen, J., Kraneveld, A.D., Keshavarzian, A., 2019. Role of TLR4 in the gut-brain axis in Parkinson's disease: a translational study from men to mice. Gut 68, 829–843. https://doi.org/10.1136/gutjnl-2018-316844

Pouclet, H., Lebouvier, T., Coron, E., des Varannes, S.B., Rouaud, T., Roy, M., Neunlist, M., Derkinderen, P., 2012. A comparison between rectal and colonic biopsies to detect Lewy pathology in Parkinson's disease. Neurobiol. Dis. 45, 305–309. https://doi.org/10.1016/j.nbd.2011.08.014

Reimer, L., Vesterager, L.B., Betzer, C., Zheng, J., Nielsen, L.D., Kofoed, R.H., Lassen, L.B., Bølcho, U., Paludan, S.R., Fog, K., Jensen, P.H., 2018. Inflammation kinase PKR phosphorylates α-synuclein and causes α-synuclein-dependent cell death. Neurobiol. Dis. 115, 17–28. https://doi.org/10.1016/j.nbd.2018.03.001

Scheperjans, F., Aho, V., Pereira, P.A.B., Koskinen, K., Paulin, L., Pekkonen, E., Haapaniemi, E., Kaakkola, S., Eerola-Rautio, J., Pohja, M., Kinnunen, E., Murros, K., Auvinen, P., 2015. Gut microbiota are related to Parkinson's disease and clinical phenotype. Mov. Disord. Off. J. Mov. Disord. Soc. 30, 350–358. https://doi.org/10.1002/mds.26069

Shan, J., Qu, Y., Wang, S., Wei, Y., Chang, L., Ma, L., Hashimoto, K., 2021. Regulation of neurotoxicity in the striatum and colon of MPTP-induced Parkinson's disease mice by gut microbiome. Brain Res. Bull. 177, 103–110. https://doi.org/10.1016/j.brainresbull.2021.09.009

Simon, D.K., Tanner, C.M., Brundin, P., 2020. Parkinson disease epidemiology, pathology, genetics, and pathophysiology. Clin. Geriatr. Med. 36, 1–12. https://doi.org/10.1016/j.cger.2019.08.002

Sulzer, D., Alcalay, R.N., Garretti, F., Cote, L., Kanter, E., Agin-Liebes, J., Liong, C., McMurtrey, C., Hildebrand, W.H., Mao, X., Dawson, V.L., Dawson, T.M., Oseroff, C., Pham, J., Sidney, J., Dillon, M.B., Carpenter, C., Weiskopf, D., Phillips, E., Mallal, S., Peters, B., Frazier, A., Lindestam Arlehamn, C.S., Sette, A., 2017. T cells from patients with Parkinson's disease recognize α-synuclein peptides. Nature 546, 656–661. https://doi.org/10.1038/nature22815

Takahashi, K., Nishiwaki, H., Ito, M., Iwaoka, K., Takahashi, K., Suzuki, Y., Taguchi, K., Yamahara, K., Tsuboi, Y., Kashihara, K., Hirayama, M., Ohno, K., Maeda, T., 2022. Altered gut microbiota in Parkinson's disease patients with motor complications. Parkinsonism Relat. Disord. 95, 11–17. https://doi.org/10.1016/j.parkreldis.2021.12.012

Tansey, M.G., Wallings, R.L., Houser, M.C., Herrick, M.K., Keating, C.E., Joers, V., 2022. Inflammation and immune dysfunction in Parkinson disease. Nat. Rev. Immunol. 22, 657–673. https://doi.org/10.1038/s41577-022-00684-6

Thomasi, B.B., de, M., Valdetaro, L., Ricciardi, M.C.G., Hayashide, L., Fernandes, A.C.M.N., Mussauer, A., da Silva, M.L., da Cunha Faria-Melibeu, A., Ribeiro, M.G.L., de Mattos Coelho-Aguiar, J., Campello-Costa, P., Moura-Neto, V., Tavares-Gomes, A.L., 2022. Enteric glial cell reactivity in colonic layers and mucosal modulation in a mouse model of Parkinson's disease induced by 6-hydroxydopamine. Brain Res. Bull. 187, 111–121. https://doi.org/10.1016/j.brainresbull.2022.06.013

Toti, L., Travagli, R.A., 2014. Gastric dysregulation induced by microinjection of 6-OHDA in the substantia nigra pars compacta of rats is determined by alterations in the brain-gut axis. Am. J. Physiol. Gastrointest. Liver Physiol. 307, G1013–G1023. https://doi.org/10.1152/ajpgi.00258.2014

Ulusoy, A., Phillips, R.J., Helwig, M., Klinkenberg, M., Powley, T.L., Di Monte, D.A., 2017. Brain-to-stomach transfer of α-synuclein via vagal preganglionic projections. Acta Neuropathol. (Berl.) 133, 381–393. https://doi.org/10.1007/s00401-016-1661-y

Van Den Berge, N., Ferreira, N., Mikkelsen, T.W., Alstrup, A.K.O., Tamgüney, G., Karlsson, P., Terkelsen, A.J., Nyengaard, J.R., Jensen, P.H., Borghammer, P., 2021. Ageing promotes pathological alpha-synuclein propagation and autonomic dysfunction in wild-type rats. Brain 144, 1853–1868. https://doi.org/10.1093/brain/awab061

Van Den Berge, N., Ferreira, N., Gram, H., Mikkelsen, T.W., Alstrup, A.K.O., Casadei, N., Tsung-Pin, P., Riess, O., Nyengaard, J.R., Tamgüney, G., Jensen, P.H., Borghammer, P., 2019. Evidence for bidirectional and trans-synaptic parasympathetic and sympathetic propagation of alpha-synuclein in rats. Acta Neuropathol. (Berl.) 138, 535–550. https://doi.org/10.1007/s00401-019-02040-w

Vaerešlija, D., Tipton, K.F., Davey, G.P., McDonald, A.G., 2020. 6-Hydroxydopamine: a far from simple neurotoxin. J. Neural Transm. 127, 213–230. https://doi.org/10.1007/s00702-019-02133-6

Wakabayashi, K., Toyoshima, Y., Awamori, K., Anezaki, T., Yoshimoto, M., Tsuji, S., Takahashi, H., 1999. Restricted occurrence of Lewy bodies in the dorsal vagal nucleus in a patient with late-onset parkinsonism. J. Neurol. Sci. 165, 188–191. https://doi.org/10.1016/S0022-510X(99)00101-X

Wang, W.-W., Han, R., He, H.-J., Li, J., Chen, S.-Y., Gu, Y., Xie, C., 2021. Administration of quercetin improves mitochondria quality control and protects the neurons in 6-OHDA-lesioned Parkinson's disease models. Aging 13, 11738–11751. https://doi.org/10.18632/aging.202868

Witoelar, A, Jansen, I.E., Wang, Y., Desikan, R.S., Gibbs, J.R., Blauwendraat, C., Thompson, W.K., Hernandez, D.G., Djurovic, S., Schork, A.J., Bettella, F., Ellinghaus, D., Franke, A., Lie, B.A., McEvoy, L.K., Karlsen, T.H., Lesage, S., Morris, H.R., Brice, A., Wood, N.W., Heutink, P., Hardy, J., Singleton, A.B., Dale, A.M., Gasser, T., Andreassen, O.A., Sharma, M., , for the International Parkinson's Disease Genomics Consortium (IPDGC), N.A.B.E.C. (NABEC), and United Kingdom Brain Expression Consortium (UKBEC) Investigators,, 2017. Genome-wide pleiotropy between Parkinson disease and autoimmune diseases. JAMA Neurol. 74, 780–792. https://doi.org/10.1001/jamaneurol.2017.0469

Zhang, X.-L., Zhang, X.-H., Yu, X., Zheng, L.-F., Feng, X.-Y., Liu, C.-Z., Quan, Z.-S., Zhang, Y., Zhu, J.-X., 2021. Enhanced contractive tension and upregulated muscarinic receptor 2/3 in colorectum contribute to constipation in 6-hydroxydopamine-induced Parkinson's disease rats. Front. Aging Neurosci. 13.

Zhu, Y., Yuan, M., Liu, Y., Yang, F., Chen, W.-Z., Xu, Z.-Z., Xiang, Z.-B., Xu, R.-S., 2022. Association between inflammatory bowel diseases and Parkinson's disease: systematic review and meta-analysis. Neural Regen. Res. 17, 344–353. https://doi.org/10.4103/1673-5374.317981

Zhurakovskaya, E., Leikas, J., Pirttimäki, T., Casas Mon, F., Gynther, M., Aliev, R., Rantamäki, T., Tanila, H., Forsberg, M.M., Gröhn, O., Paasonen, J., Jalkanen, A.J., 2019. Sleep-state dependent alterations in brain functional connectivity under urethane anesthesia in a rat model of early-stage Parkinson's disease. eNeuro 6https://doi.org/10.1523/ENEURO.0456-18.2019. ENEURO.0456-18.2019.